PAPER

Check for updates

Icariin controlled release on a silk fibroin/mesoporous bioactive glass nanoparticles scaffold for promoting stem cell osteogenic differentiation†

Xiaofeng Shen,‡ Pengfei Yu,‡ Hua Chen,‡ Jiangping Wang, Binjie Lu, Xuefeng Cai, Chun Gu, Guoqiang Liang, Donglin Hao, Qihan Ma* and Yuwei Li [ID] *

The treatment of bone defects caused by various reasons is still a major problem in orthopedic clinical work. Many studies on osteogenic implant materials have used various biologically active factors such as osteogenic inducers, but these biologically active factors have various side effects. Therefore, in this study, silk fibroin (SF) was used as a scaffold material, mesoporous bioactive glass nanoparticles (MBGNs) as a sustained release carrier, and the traditional Chinese drug icariin (ICA) was loaded to promote bone formation. The experiments in this study have proven that SF/MBGNs-ICA scaffolds can successfully load and release ICA for a long time, and the sustained-release ICA can promote the proliferation and differentiation of BMSCs for a long time. This controlled-release ICA organic/inorganic two-component scaffold material is expected to become a new bone grafting solution.

1. Introduction

At present, the treatment of bone defects caused by various reasons is still a major problem in orthopedic clinical work.[1,2] Among the existing bone graft materials, autogenous bone grafting is the gold standard, but there are limitations such as insufficient supply and complications in the donor site, allogeneic or xenogeneic bones have risks such as immune rejection and viral transmission.[1–3] Although the research on scaffold materials in the field of biomaterials has been deepened, there are still some problems in biocompatibility, and osteoinductive and osteogenic properties have not been solved.[4]

Silk fibroin (SF) is a natural polymer fibrin extracted from natural silk. In recent years, SF has attracted attention in the field of tissue engineering due to its good biocompatibility, strong mechanical properties, and ease of processing.[5,6] There have also been many studies using silk fibroin to prepare films, gels, electrospinning membranes, particles, *etc.* for different tissue regeneration.[7] Among them, silk fibroin scaffolds have attracted widespread attention in the field of osteogenic materials due to their good mechanical properties, adjustable degradation ability, and ability to promote the adhesion and proliferation of MSCs.[8] However, the components of bone are 1/3 organic and 2/3 inorganic. The stent of organic components

cannot match the regeneration of bone tissue. At the same time, many studies have also showed that inorganic ions such as silicon and calcium are not only able to promote the formation of hydroxyapatite layers in the body, but also directly promote the proliferation and differentiation of osteoblasts.[9]

Bioactive glass (BG) has excellent osteoconductivity, osteoinduction, and biocompatibility.[10] Among them, mesoporous bioactive glass nanoparticles (MBGNs) have a large specific surface area and a unique mesoporous structure, which can release ions in body fluids, promote the production of surface-active HAC and genes related with bone formation, so it is also favored as a bone-promoting inorganic material.[11] However, the macroscopic morphology of MBGNs particles is powdery, which is difficult to be formed. It has the disadvantages of large brittleness, low elastic modulus, and inability to be used in load bearing parts. Therefore, combining MBGNs with silk fibroin scaffolds is an ideal choice to prepare direct materials that are similar in composition to natural bone tissue.

However, it takes a lone time for MBGNs to degrade and release ions in the body fluid environment. Therefore, many studies considered MBGNs as carriers for various drugs to promote cell proliferation and differentiation.[12] Most of these drugs are active biological factors. These factors have the disadvantages of poor stability *in vitro*, easy degradation and inactivation, and high local concentrations that easily lead to serious inflammatory reactions.[13,14] Icariin (ICA) is an active natural flavone glycoside extracted from Epimedium. Studies have confirmed that ICA works not only on bones by promoting osteoblast formation (causing bone formation), but also by inhibiting osteoclast formation (inhibiting bone resorption).[15] Studies have shown that ICA can promote osteogenic

Suzhou TCM Hospital Affiliated to Nanjing University of Chinese Medicine, No. 889, West Wuzhong Road, Suzhou, Jiangsu, 215009, P. R. China. E-mail: ma_zyy@126. com; lyw97538@hotmail.com

† Electronic supplementary information (ESI) available. See DOI: 10.1039/d0ra00637h

‡ These authors contributed equally to this paper.

differentiation and proliferation of MC3T3 and BMSCs to promote osteogenesis.[16]

Therefore, in this study, MBGNs were used to load ICA, and MBGNs-ICA was compounded into silk fibroin scaffolds to obtain SF/MBGNs-ICA scaffolds to achieve the purpose of ICA controlled releasing. At present, some studies have used organic–inorganic composite scaffolds to adsorb ICA to promote the repair of bone tissue. For example, Xie *et al.*[17] use icariin-loaded hydroxyapatite/ alginate (IC/HAA) porous composite scaffolds to slow release ICA. Lai *et al.*[18] use poly(lactic-*co*-glycolic acid)/b-calcium phosphate/ icariin (PLGA/TCP/icariin, PTI) 3D print scaffold to achieve the purpose of bone formation, Reiter *et al.*[19] use gelatin-coated, 3D sponge-like scaffolds to load ICA. Compared with these studies, in this study, bioactive glass nanoparticles with mesoporous structure were used to load and release ICA, therefore, this novels scaffold material have higher loading capacity and long-term sustained-release performance. At the same time, larger specific surface area of MBGNs than other inorganic materials could provide stronger ability to promote the formation of hydroxyapatite layer in body fluid environment. In this study, the onlooking morphology of SF/MBGNs-ICA scaffolds and the controlled release capacity of ICA were characterized. At the same time, the osteogenic ability of the scaffolds was evaluated through *in vitro* cell adhesion, proliferation, toxicity, and differentiation experiments.

2. Experimental section

2.1. Preparation and characterization of drug loaded MBGNs

MBGNs were synthesized using cetyltrimethylammonium bromide (CTAB, Sigma-Aldrich, USA) as the template and Tris–HCl buffer (pH = 8) as the catalyst.[20] The detailed process is listed in the ESI.†

5 mg of ICA (Aladdin, China) was dissolved in 5 ml of ethanol, and 10 mg MBGNs were added. After being vacuumed and stirred overnight, MBGNs adsorbed ICA, washed and freeze-dried for further characterization. The particle size and microscopic morphology of MBGNs and MBGNs-ICA were observed using a transmission electron microscope (TEM).

2.2. Preparation and characterization of SF/MBGNs-ICA scaffold

Silk fibroin (SF) was obtained from the cocoons of *B. mori* silkworm (Rudong Xinsilu Co., Ltd., Jiangsu, China), the silk solution were prepared as previously described.[8] The detailed process is listed in the ESI.†

Inject 30 µl of 6% (w/v) silk fibroin solution into the template (5 mm in diameter and 2 mm in height), freeze-dry for 48 h, treat with methanol for 0.5 h, wash with deionized water for 1 h, and freeze-dry again to obtain the pure SF scaffold, namely the Control group. Add 1% MBGNs microspheres (10 mg:1 ml) to a 6% silk fibroin solution, sonicate, and take 30 µl of the mixed solution into the template (diameter 5 mm, height 2 mm), freeze-dry for 48 h, and then treat with methanol 0.5 h, washed with deionized water for 1 h, and lyophilized again to obtain the SF/MBGNs composite scaffold, namely the S/M group. 5 mg of ICA was dissolved in 5 ml of ethanol, and the prepared SF or SF/

MBGMs (5 pieces for each group) scaffold was put into the solution. After being vacuumed and stirred overnight, the scaffold was adsorbed to ICA, washed and freeze-dried to obtain SF-ICA (abbreviated as SF-I) scaffold and SF/MBGNs-ICA (here-inafter abbreviated as SF/M-I) scaffold, the centrifugal super-natant and washing solution were kept for concentration detection, and the remaining ICA concentration was measured by high performance liquid chromatography (HPLC, Varian Prostar240, USA). After the reaction and washed solution was measured for concentration by HPLC, it was calculated that an average piece of SF scaffold material adsorbed 115 µg ICA, and a piece of SF/MBGNs could adsorb 120 µg ICA in average.

The chemical structure of the scaffold was scanned by Fourier transform infrared spectroscopy (FTIR, Nicolet 6700; Thermo scientific, USA). The morphology of the silk fibroin scaffold was observed using a scanning electron microscope (SEM, S-4800; Hitachi, Tokyo, Japan). In order to test the sustained release performance of ICA in the scaffold, composite scaffolds of different groups ($n = 3$) were placed in 5 ml centrifuge tubes, 2 ml of PBS was added, and they were shaken in a 37 °C constant temperature shaker. At the specified time point (0, 2, 4, 8, 12, 24 d), take out as much liquid as possible and add new 2 ml PBS. The obtained liquid was subjected to HPLC detection, and the obtained result was plotted as a release curve.

2.3. Cell adhesion, proliferation and viability test

5×10^3 cells in 200 µl of medium were planted in each scaffold, and the culture plate was placed in an incubator at 37 °C, 95% humidity and 5% CO_2, and the solution was changed every two days. After 7 days of culture, fixing and dehydration, then observe the cell morphology and take pictures under a 10 kV voltage using SEM. Cell proliferation was measured using cell counting kit-8 reagent (CCK-8, Dojindo, Kumamoto, Japan). At the specified time (1 d, 3 d, 5 d, and 7 d), the scaffolds with BMSCs seeded were incubated in 10% (v/v) CCK-8 solution at 37 °C with 5% CO_2 for 2 h. The obtained solution was measured at 450 nm using a spectrophotometer. In order to test the toxicity of different groups scaffolds, cells were cultured in the manner and quantity described above, and after 14 days of culture, the cells were stained with Live-Dead staining kit to observe the number live cells and dead cells.

2.4. Cells mineralization *in vitro*

Before detecting the ALP activity, calcium nodule formation and gene expressions, the BMSCs were seeded in the lower chamber in the 24-well plate, and the scaffolds were put into the upper chamber. Osteogenic induction medium (OM, Cyagen, Guangzhou, China) was used to culture the cells.

After 7 d, the cells were fixed with 4% paraformaldehyde, followed by ALP staining (Biosharp, China) for 20 min. The ALP positive cells were stained blue.

After 21 d, the cells were fixed with 4% paraformaldehyde, followed by staining with Alizarin Red S (ARS) staining kit (Cyagen, Guangzhou, China) for 15 min. Wash the cells again with deionized water and observe under a microscope. In order to quantitatively determine the amount of calcium nodule

Paper

deposition, 1 ml of 10% cetylpyridine chloride was added to each well of the culture plate that had been stained, and the Alizarin Red was completely dissolved by reacting for 1 h at room temperature. The absorbance was then measured at 562 nm and recorded.

2.5. Immunofluorescence staining of osteogenic differentiation of cells

After 21 days, cells were fixed with 4% paraformaldehyde for 10 min, permeabilized with 0.5% Triton X-100 (Sigma-Aldrich, USA), and blocked with 1% BSA (Solarbio, Beijing, China). After washing with PBS, cells were soaked in OCN primary antibody (Abcam, USA) at 4 °C and incubated overnight. After washing with PBS the next day, cells were incubated in goat anti-mouse IgG H&L (Abcam, USA) secondary antibody at 37 °C for 1 h, and the nuclei were stained with DAPI.

2.6. Expression of osteogenic genes

The expression of Alp, Runx2, Opn, and Ocn were analyzed by quantitative reverse transcription polymerase chain reaction (RT-qPCR). The RT-qPCR assay was performed to evaluate the expression levels of the genes of BMSCs cultured with the scaffold at 3, 7 and 14 d.[21] The primer sequences used for PCR amplification are listed in Table 1. Glyceraldehyde-3-phosphate dehydrogenase (Gapdh) was used as an internal control, and all primers were synthesized by Invitrogen.

2.7. Statistical analysis

All data were analyzed with GraphPad Prism 8 software (GraphPad, Inc., La Jolla, CA, USA) to determine statistical significance and are reported as the mean ± SD. One-way analysis of variance (ANOVA) and Tukey's method for multiple comparisons were used to evaluate differences in motility and gene expression across three or more treatment groups.

3. Results and discussion

3.1. Preparation and characterization of drug loaded MBGNs and SF/MBGNs-ICA scaffold

Bio-active scaffolds loaded with drugs to induce bone growth have become more mature treatments for bone defects. Many traditional Chinese medicines have the advantages of stable chemical structure and low immune response. The purpose of this study is to use the silk fibroin scaffold as a microenvironment for cell growth and use the controlled-release icariin to promote the adhesion, proliferation and differentiation of osteoblasts. In order to achieve the purpose of controlling the sustained release of icariin, in this study, MBGNs, which have high biocompatibility and can also promote bone formation, were used as the carrier of ICA.

Fig. 1A showed that the general appearance of MBGNs is white powder, and the general appearance of ICA is yellow powder. The TEM results of MBGNs in Fig. 1B showed that MBGNs are regular spherical and have a channel structure inside. The diameter of MBGNs measured by measurement is 103.8 ± 6.4 nm. After MBGNs adsorbed ICA in ethanol solution immersed in ICA, the channel structure was slightly blurred. The MBGNs synthesized by this synthesis method have ordered mesoporous pores and have a large specific surface area. The particle size distribution is also relatively uniform, and it can release silicon, calcium, and phosphorus ions in a physiological environment.[22] TEM confirmed that MBGNs are regular spherical particles of uniform size. However, there are some disadvantages when MBGNs are used alone as a carrier or scaffold, such as poor mechanical properties, high brittleness, and it is difficult to match the degradation rate with the new bone growth rate.[23] Therefore, MBGNs are often used as particle-reinforced phases to compound with polymer materials to prepare inorganic-phase particles/organic composites with nano-scale size effects to enhance the mechanical and biological properties of the materials and provide effective growth space for cell and tissue regeneration.

The preparation process of ICA-adsorbed SF/MBGNs scaffold is shown in Fig. S1,† and the SEM morphology of synthetic SF and SF/MBGNs scaffolds is shown in Fig. 1C. The morphology of silk fibroin scaffolds was irregular and porous. The pore diameter of the scaffolds was 54.2 ± 8.1 μm. After MBGNs were added, the pore diameter was reduced to about 36.2 ± 9.3 μm. However, when observed at a magnification of 3000, it is obvious that the pore wall of the SF group is smoother, while MBGNs particles are attached to the pore wall of the SF/MBGNs group (indicated by yellow arrows), indicating that MBGNs particles can be uniformly attached in the SF scaffold. The FTIR

Table 1 Primers used for RT-qPCR

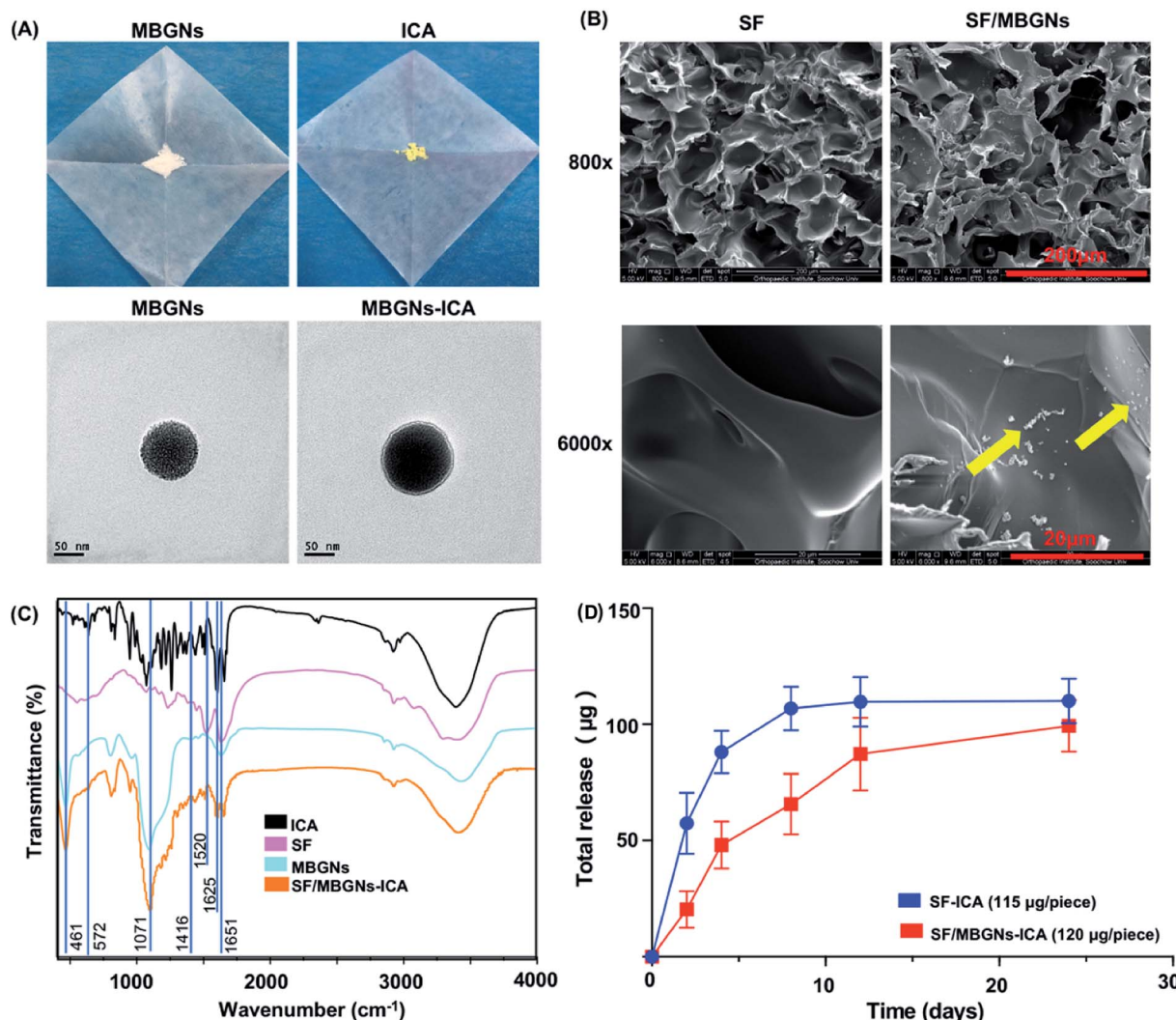| Gene	Primer/probe	Sequence	Ann. temp T_m (°C)
Alp	Forward	CGTCTCCATGGTGGATTATGCT	64.5
	Reverse	CCCAGGCACAGTGGTCAAG	
Runx2	Forward	TCTTCCCAAAGCCAGAGCG	64.5
	Reverse	TGCCATTCGAGGTGGTCG	
Opn	Forward	GAGGAGAAGGCGCATTACAG	57
	Reverse	AAACGTCTGCTTGTCTGCTG	
Ocn	Forward	CATGAAGGCTTTGTCAGACT	57
	Reverse	CTCTCTCTGCTCACTCTGCT	
Gapdh	Forward	GGCAAGTTCAACGGCACAGT	57 and 64.5
	Reverse	GCCAGTAGACTCCACGACAT	

Fig. 1 (A) General morphology of MBGNs and ICA, (B) SEM images of SF scaffold (scale bar = 200 μm) and high magnification (scale bar = 50 μm) with ratio of MBGNs 1% wt, (C) FTIR spectra of ICA, SF, MBGNs and SF/MBGNs-ICA, (D) ICA releasing from SF-ICA and SF/MBGNs-ICA.

spectra of SF, ICA, SF/MBGNs and SF/MBGNs-ICA scaffolds are shown in Fig. 1D. The peaks at 1650 cm^{-1} (amide I) and 1416 cm^{-1} (amide II) correspond to the SF, the existence of MBGNs in the SF scaffold is confirmed by the appearance of a peaks at 461 cm^{-1} and 1071 cm^{-1}, which are ascribed to the Si–O–Si characteristic peaks, and its intensity changed little with the addition of the MBGNs loaded with ICA. The peaks at 572 cm^{-1} correspond to the glycosidic bond in ICA, prove the successful load of ICA.

The *in vitro* release shown in Fig. 3A. There was a release with 49.4% of the total ICA released from the pure SF scaffolds in the first 2 days, it was slowed down with 92.8% of the total ICA released after 8 d. In contrast, the overall release of ICA from the SF/MBGNs-ICA scaffold was comparatively slow and sustained compared with pure SF scaffold, 16.9% of the total ICA released from the pure SF scaffolds in the first 2 days and 54.7% of the total ICA released after 4 d, 73% after 8 d.

SEM results showed that the composite SF scaffold still has a good porous structure, and MBGNs can be distributed in the scaffold. The appearance of characteristic peaks related to glycosidic bonds in FTIR results proves the effective load of ICA in MBGNs in SF scaffolds, and the porous structure of SF scaffolds is also conducive to maintaining a certain local concentration of ICA after sustained release, which is beneficial for ICA to perform a pharmacological action to the cells attached on the scaffold. After HPLC calculation, the drug loading rate of ICA by SF scaffold alone is only 87.2%, and the drug loading rate of SF/MBGNs by ICA reached to 93.3%, which may be related to the strong adsorption capacity of MBGNs. In the subsequent sustained release experiments, we observed that the ICA concentration in the pure SF scaffold group was very low on day 8 and the release was basically complete, while the release in the SF/MBGNs group could continue until day 24. A similar process has been reported by Lazzara *et al.*[24] to achieve protein lag release by immobilizing protein adsorption in a palisade matrix by a release–resorption–rerelease progress.
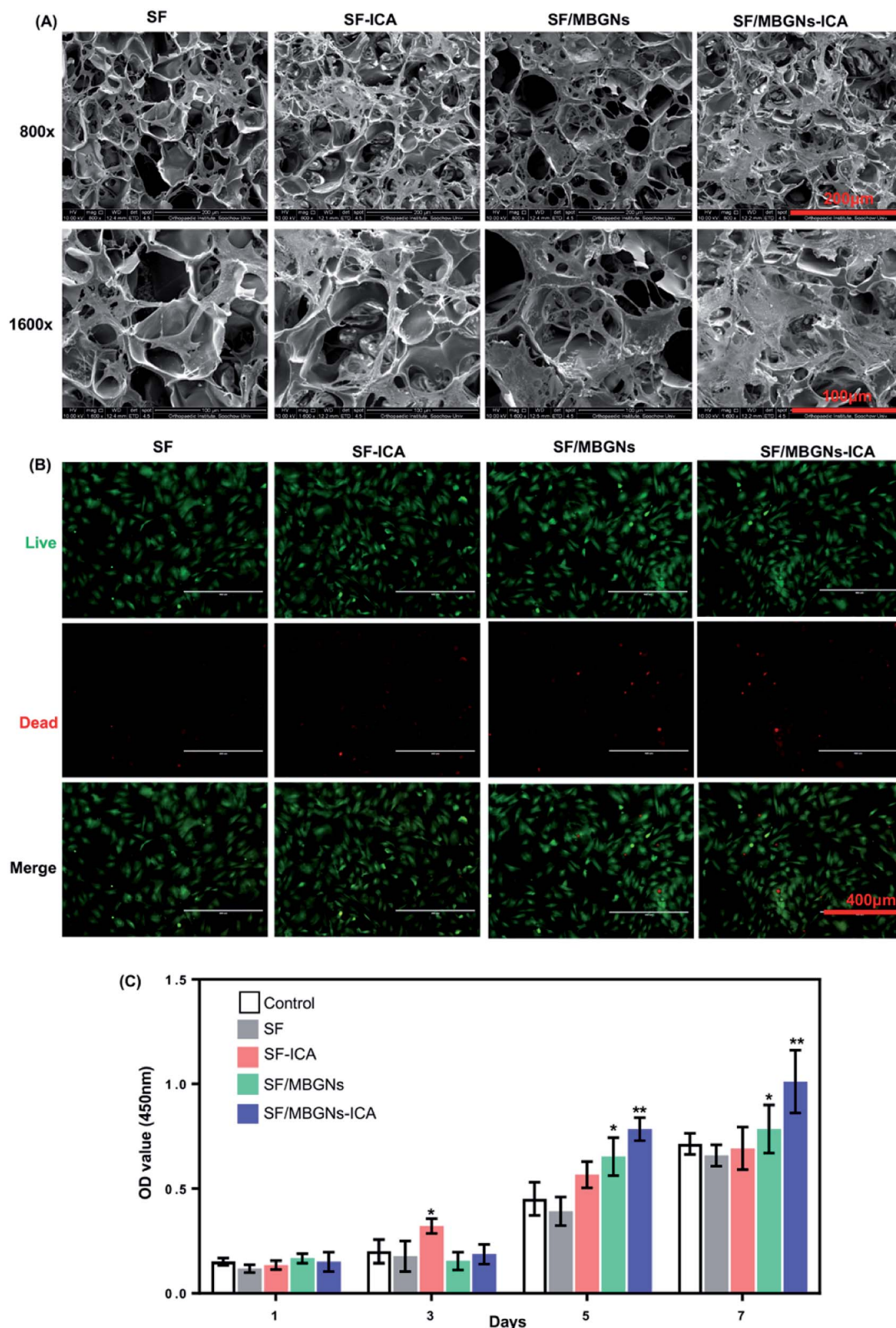
Fig. 2 Cell adhesion, cytotoxicity assays and proliferation: (A) the SEM images of cells on the scaffold after seeding for 7 d, (B) the live–dead staining of cells cultured after 14 d, (C) CCK-8.

3.2. Cell adhesion and viability

BMSCs seeded onto the scaffold and ultrastructural analysis was performed by scanning electron microscope (SEM) when cultured for 7 d. BMSCs were well attached and integrated with scaffolds (Fig. 2A). It showed that the scaffold material was covered by more spreading and the cell morphology was all
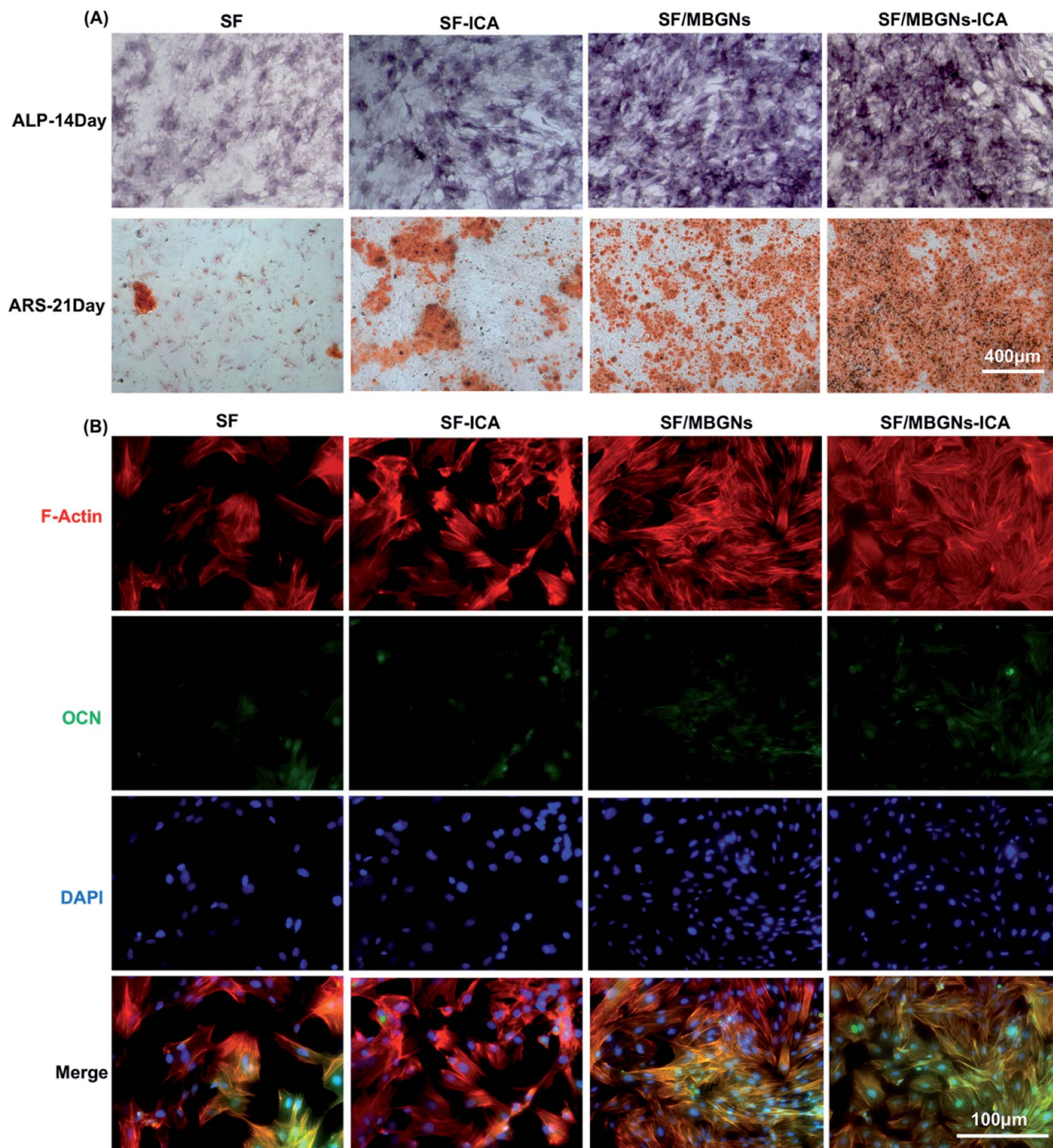
Fig. 3   Osteogenesis of BMSCs measured by (A) ALP staining at 7 d and Alizarin Red staining at 21 d. Scale bar = 400 μm. (B) Immunofluorescence assays for OCN expression at 14 d, with the nucleus stained in blue (DAPI) and OCN stained in red. Scale bar = 100 μm.

covered by spindle-shaped stretching until the 7th day of culture, which proved that the silk fibroin scaffold materials had good biocompatibility. And by the 7 d, the number of cells in the SF-ICA scaffold was slightly more than that of the pure SF scaffold, but the number of cells on the two groups of scaffold materials was less than the latter two groups with MBGNs added, and the SF/MBGNs-ICA group was covered with largest number of cells. The cell number comparisons of 1, 3, 5 and 7

days were tested using the CCK-8 kit. The results are shown in Fig. 2C. The experimental results showed that the addition of MBGNs and ICA can effectively promote the proliferation of BMSCs.

The toxicity test of scaffold release on BMSCs was performed using Transwell plates and live-dead staining. Live-dead staining was performed after 14 days of culture (Fig. 2B). It was proved that the silk fibroin scaffold with or without MBGNs and

ICA had little effect on cell viability. Cell SEM results showed that BMSCs can adhere and proliferate well on silk fibroin scaffolds. The cell proliferation results quantified by CCK-8 also confirm this, because the loose porous structure of silk fibroin scaffolds can not only provide natural ECM for cells, a good growth scaffold environment is also conducive to nutrient and gas exchange between cells and the surrounding environment. Since MBGNs degradation takes a long time, even when ICA release is completed after 24 days, MBGNs continue to degrade. Still able to maintain cell proliferation. Huang et al.[25] showed that ICA can effectively prevent femoral head necrosis, improve prednisolone-induced BMSC proliferation, enhance osteoblastic differentiation, and inhibit adipogenic differentiation. In addition, low concentrations of ICA (10^{-9} M to 10^{-5} M) significantly increased BMSC proliferation, especially at 10^{-6} M.[26] The release experiment proved that the solution concentration of ICA can still reach 10^{-6} M by the 24th day. There are also reports that when the concentration of ICA is greater than 10^{-5} M, significant cytotoxicity will be produced,[27] however, during the sustained release of ICA, only the drug concentration on the 1st day exceeded 10^{-5} M.

3.3. Osteogenic differentiation of cells *in vitro*

After 14 days of cell induction, ALP activity was measured. As shown in Fig. 3A, the SF/MBGNs group and the SF/MBGNs-ICA group have significantly more ALP staining, and the ALP expression in the SF/MBGNs-ICA group is the most intense than the other groups.

After 21 days of cell induction, the content of calcium nodules was measured. As shown in the Fig. 3A, the MBGNs-containing group was more stained with Alizarin Red than the SF and SF-ICA groups, and the SF/MBGNs-ICA group had more calcium nodules. The Alizarin Red quantized results of calcium nodule staining (Fig. S2†) suggest that nanoparticle slow-release ICA and MBGNs have a synergistic effect on promoting osteogenic differentiation of cells, while pure silk fibroin scaffolds have no significant effect on promoting osteogenic differentiation.

OCN immunofluorescence staining was performed at 21 days' induction culture, and the results are shown in Fig. 3B. The results are similar to the calcium nodule staining appeal. The expression levels of OCN in MBGNs group and SF/MBGNs-ICA group were significantly higher than those in SF group and SF-ICA group, and the expression in SF/MBGNs-ICA group was more obvious.

Finally, we performed RT-qPCR detection on the four osteogenic related genes: Alp, Runx2, Ocn and Opn at 3, 7 and 14 days, as shown in Fig. 4, as markers of early osteogenic genes, the expression of ALP and Runx2 was similar. After 3 days' culture, the expression of ALP and Runx2 in the SF-ICA group, SF/MBGNs-ICA group were higher than those in the other two groups. After 7 days' culture, the expression in SF group began to be lower than other groups, but the expression level in SF-ICA group was higher, which may be related to the early rapid ICA release. The expression of Ocn and Opn continued to rise as late markers of osteogenic, and the expression in groups containing ICA were also higher than the other three groups. At the same time, the expression in the SF/MBGNs-ICA group also began to be higher than SF-ICA and SF/MBGNs group after 7 d. In order to verify the above-mentioned *in vitro* osteogenic differentiation results, we performed immunofluorescence staining and PCR experiments. The PCR results at 3 and 7 days showed high
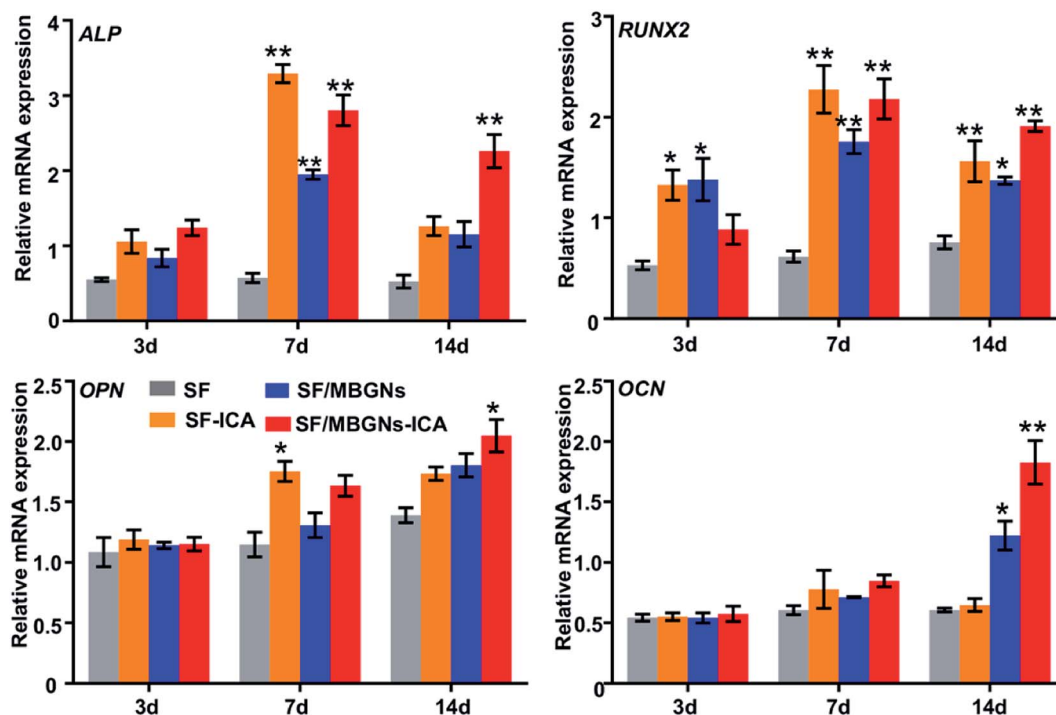

Fig. 4 Detection of mRNA from selected osteogenic markers in BMSCs after 3 d, 7 d, and 14 d of incubation. The mRNA levels of Alp, Runx2, Opn, and Ocn were quantified ($*p < 0.05$ and $**p < 0.01$ compared with control).

expression of osteogenesis-related genes in the SF-ICA group, which also confirmed the early burst release of ICA, which is consistent with the results of *in vitro* release. ICA has multiple pharmacological activities, including hormone-like, antitumor, immunomodulatory, and antioxidative effects.[28–30] Studies have shown that ICA-mediated osteogenesis is related to its hormone-like function.[31,32] It can induce BMP-2 and BMP-4 mRNA expression in osteoblasts and significantly up-regulate Osx at low doses.[33] In addition, ICA facilitates bone formation by inducing preosteoblastic genes like Osx, Runx2, alkaline phosphatase (ALP), and collagen type I. The results in the release experiments also support and prove that this controlled-release system can slowly release ICA *in vitro* and effectively promote osteogenic differentiation of BMSCs.

4. Conclusion

The combination of SF with ICA loaded MBGNs is a competitive approach to make novel scaffolds for orthopedic applications. In this study, MBGNs loaded with ICA was successfully fabricated by adsorption technology. The MBGNs incorporation enhanced the adhesive properties of SF scaffold. Cell culture and CCK-8 assay indicated that the SF/MBGNs-ICA scaffold had good cell affinity and cytocompatibility. ICA and ions released from the scaffold synergistically promote cell proliferation and differentiation. In the future, we will make some further study to illustrate the potential and promise of SF/MBGNs-ICA scaffold *in vivo*.

Conflicts of interest

The authors declare no conflicts of interest.

Acknowledgements

References

1 R. Dimitriou, E. Jones, D. Mcgonagle and P. V. Giannoudis, *BMC Med.*, 2011, **9**, 66.

2 D. Tang, R. S. Tare, L. Y. Yang, D. F. Williams and R. O. C. Oreffo, *Biomaterials*, 2016, **83**, 363–382.

3 Z. Li, M. B. Xie, Y. Li, Y. Ma, J. S. Li and F. Y. Dai, *J. Biomater. Tissue Eng.*, 2016, **12**, 755–766.

4 R. Langer, *Adv. Mater.*, 2009, **21**, 3235–3236.

5 M. Y. Yang, *Microsc. Res. Tech.*, 2017, **80**, 321–330.

6 L. Meinel, S. Hofmann, V. Karageorgiou, C. Kirker-Head, J. McCool, G. Gronowicz, L. Zichner, R. Langer, G. Vunjak-Novakovic and D. L. Kaplan, *Biomaterials*, 2005, **26**, 147–155.

7 J. Melke, S. Midha, S. Ghosh, K. Ito and S. Hofmann, *Acta Biomater.*, 2015, **31**, 1–16.

8 H. Liu, G. W. Xu, Y. F. Wang, H. S. Zhao, S. Xiong, Y. Wu, B. C. Heng, C. R. An, G. H. Zhu and D. H. Xie, *Biomaterials*, 2015, **49**, 103–112.

9 O. Mahony, O. Tsigkou, C. Ionescu, C. Minelli, L. Ling, R. Hanly, M. E. Smith, M. M. Stevens and J. R. Jones, *Adv. Funct. Mater.*, 2010, **20**, 3835–3845.

10 L. L. Hench, R. J. Splinter, W. C. Allen and T. K. Greenlee, *J. Biomed. Mater. Res.*, 1971, **5**(6), 117–141.

11 D. Zhao, J. Feng, Q. Huo, N. Melosh, G. H. Fredrickson, B. F. Chmelka and G. D. Stucky, *Science*, 1998, **279**, 548–552.

12 M. Yu, Y. Xue, P. X. Ma, C. Mao and B. Lei, *ACS Appl. Mater. Interfaces*, 2017, **9**, 8460–8470.

13 A. Arzeno, T. Wang and R. J. Huddleston, *Arthroplasty Today*, 2018, **4**(2), 162–168.

14 J. N. Zara, R. K. Siu, X. Zhang, J. Shen and C. Soo, *Tissue Eng., Part A*, 2011, **17**, 1389–1399.

15 P. Yang, Y.-Q. Guan, Y.-L. Li, L. Zhang, L. Zhang and L. Li, *Mol. Med. Rep.*, 2016, **14**, 1316–1322.

16 L. Song, J. Zhao, X. Zhang, H. Li and Y. Zhou, *Eur. J. Pharmacol.*, 2013, **714**, 15–22.

17 Y. Xie, W. Sun, F. Yan, H. Liu, Z. Deng and L. Cai, *Int. J. Nanomed.*, 2019, **14**, 6019–6033.

18 Y. Lai, H. Cao, X. Wang, S. Chen, M. Zhang, N. Wang, Z. Yao, Y. Dai, X. Xie, P. Zhang, X. Yao and L. Qin, *Biomaterials*, 2018, **153**, 1–13.

19 T. Reiter, T. Panick, K. Schuhladen, J. A. Roether, J. Hum and A. R. Boccaccini, *Bioact. Mater.*, 2019, **4**, 1–7.

20 T. Xin, Y. Gu, R. Cheng, J. Tang, Z. Sun, W. Cui and L. Chen, *ACS Appl. Mater. Interfaces*, 2017, **9**, 41168–41180.

21 R. A. Perez, J.-H. Kim, J. O. Buitrago, I. B. Wall and H.-W. Kim, *Acta Biomater.*, 2015, **23**, 295–308.

22 A. El-Fiqi, J. H. Lee, E.-J. Lee and H.-W. Kim, *Acta Biomater.*, 2013, **9**, 9508–9521.

23 M. Vallet-Regí and E. Ruiz-Hernández, *Adv. Mater.*, 2011, **23**, 5177–5218.

24 T. D. Lazzara, I. Mey, C. Steinem and A. Janshoff, *Anal. Chem.*, 2011, **83**, 5624–5630.

25 Z. Huang, C. Cheng, C. Beibei, W. Jing, W. Hui, L. Xianzhe, H. Yu, Y. Shuhua and W. Xiang, *Cell. Physiol. Biochem.*, 2018, **47**, 694–706.

26 F. Jun-Jun, C. Liang-Guo, W. Tao, W. De-Xin, J. Dan, J. Shan, Z. Zhi-Yong, B. Long and P. Guo-Xian, *Molecules*, 2011, **16**, 10123.

27 Z. Wang, D. Wang, D. Yang, W. Zhen, J. Zhang and S. Peng, *Osteoporosis Int.*, 2017, **29**, 535–544.

28 Z. Wang, X. Zhang, H. Wang, L. Qi and Y. Lou, *Neuroscience*, 2007, **145**, 911–922.

29 J. Zhou, J. Wu, X. Chen, N. Fortenbery, E. Eksioglu, K. N. Kodumudi, E.-B. PK, J. Dong, J. Y. Djeu and S. Wei, *Int. Immunopharmacol.*, 2011, **11**, 890–898.

30 J. Guo, F. Li, Q. Wu, Q. Gong, Y. Lu and J. Shi, *Phytomedicine*, 2010, **17**, 950–955.

31 S. S. C. Wing, T. Yao, N. T. Bun, C. C. L. Yin and C. H. Pan, *Molecules*, 2010, **15**, 7861–7870.

32 L. Qin, T. Han, Q. Zhang, D. Cao, H. Nian, K. Rahman and H. Zheng, *J. Ethnopharmacol.*, 2008, **118**, 270–279.

33 J. Zhao, S. Ohba, M. Shinkai, U. Chung and T. Nagamune, *Biochem. Biophys. Res. Commun.*, 2008, **369**, 444–448.